JOC The Journal of Organic Chemistry

Featured Article

pubs.acs.org/joc

Double Alkylene-Strapped Diphenylanthracene as a Photostable and Intense Solid-State Blue-Emitting Material

Yutaka Fujiwara,[†] Ryota Ozawa,[†] Daiki Onuma,[†] Kengo Suzuki,[‡] Kenji Yoza,[§] and Kenji Kobayashi*[,†]

[†]Department of Chemistry, Faculty of Science, Shizuoka University, 836 Ohya, Suruga-ku, Shizuoka 422-8529, Japan

[‡]Hamamatsu Photonics K. K., 812 Joko-cho, Higashi-ku, Hamamatsu 431-3196, Japan

[§]Bruker AXS, 3-9-B Moriya, Kanagawa-ku, Yokohama 221-0022, Japan

Supporting Information

ABSTRACT: We report the synthesis and photochemical and photophysical properties of double alkylene-strapped 9,10-diphenylanthracene derivatives **3a**–**c** (**a**: C6 strap, **b**: C7 strap, **c**: C8 strap) in which the reactive central aromatic ring of the anthracene moiety is protected by the double alkylene straps. Thus, **3a**–**c** were much more resistant to photochemical reactions than the parent 9,10-diphenylanthracene (DPA). Furthermore, **3b** in C_6H_{12} as well as in a cast film and the powder state showed the highest fluorescence quantum yields among **3a**, **3b**, quadruple triethylsilyl-protected DPA **4**, and DPA, wherein the C7 strap in **3b** effectively serves to block fluorescence self-quenching.

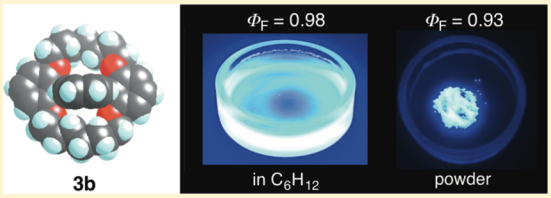

INTRODUCTION

Anthracene, 9,10-diphenylanthracene (DPA), and their derivatives are highly fluorescent materials. They are useful building blocks for optoelectronics such as organic electroluminescent devices[1] and two-photon absorption fluorescent dyes[2] and for organic semiconductors such as organic field-effect transistors[3,4] and organic photoconductors.[5] However, it is well-known that anthracene derivatives react under photoirradiation to afford photodimerization and/or photooxidation products.[6] These photochemical reactions of anthracene derivatives are disadvantageous for the purpose of uses related to photoluminescence and optoelectronics. Another problem of anthracene derivatives is fluorescence self-quenching in the solid state, caused by self-absorption with a small Stokes' shift and/or self-aggregation.[7] Recently, two main strategies for molecular designs to overcome these problems have been reported. One is a supramolecular encapsulation strategy,[8,9] and the other is a steric protection strategy.[7,8a] Yamaguchi et al. reported intense solid-state blue emission of a DPA derivative by an intramolecular π-stacking protection based on steric protection as well as rigidification of the conformation, which would suppress the nonradiative decay process from the excited state and make the radiative process more dominant.[7] An alkylene-strap method[10−12] may be another effective and simpler approach to steric protection as well as conformational rigidification of DPA. Herein, we report the synthesis and photochemical and photophysical properties of double alkylene-strapped 9,10-diphenylanthracene (DPA) derivatives **3a**–**c** (Chart 1; **a**, C6 strap; **b**, C7 strap; **c**, C8 strap) that are resistant to photochemical reactions in solution and fluorescence self-quenching in the solid state.

Chart 1. Structures of 1, 2, Double Alkylene-Strapped DPAs 3a–c, Quadruple Triethylsilyl-Protected DPA 4, and DPA

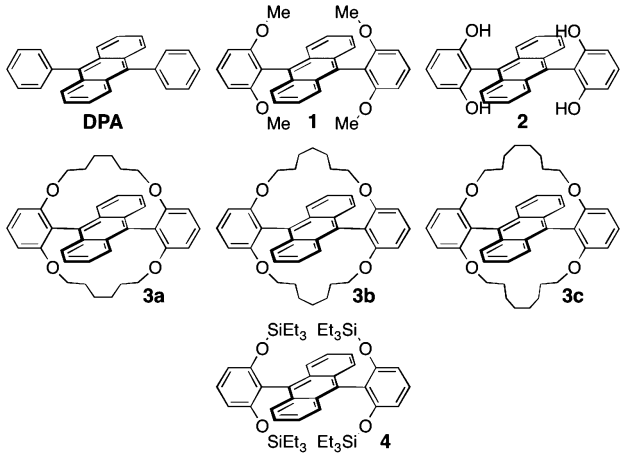

RESULTS AND DISCUSSION

Synthesis. Double alkylene-strapped DPAs **3a**–**c** (**a**, C6 strap; **b**, C7 strap; **c**, C8 strap) were synthesized following a four-step or three-step procedure (Scheme 1). The reaction of anthraquinone with 2,6-dimethoxyphenyllithium[13] followed by the dehydroxy aromatization of the resulting diol with NaI–NaH_2PO_2–AcOH[14] or the Suzuki–Miyaura cross-coupling reaction[13] of 9,10-dibromoanthracene with 2,6-dimethoxyphenylboronic acid gave 9,10-bis(2,6-dimethoxyphenyl)anthracene

Received: December 1, 2012
Published: January 16, 2013

   dx.doi.org/10.1021/jo302621k | J. Org. Chem. 2013, 78, 2206–2212

Scheme 1. Synthesis of 1, 2, 3a–c, and 4[a]

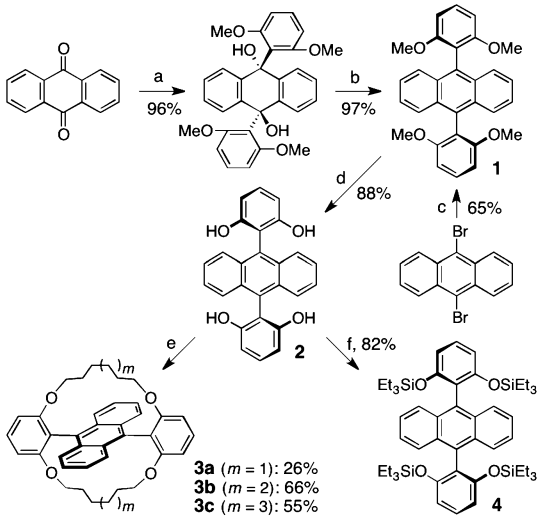

[a]Key: (a) 2,6-dimethoxyphenyllithium, THF, −78 °C to rt; (b) NaI, $NaH_2PO_2{\cdot}H_2O$, AcOH, 120 °C; (c) 2,6-dimethoxyphenylboronic acid, $Pd(OAc)_2$, SPhos,[13] K_3PO_4, THF–H_2O, 60 °C; (d) BBr_3, CH_2Cl_2, −78 °C to rt; (e) 1,*n*-Dibromoalkane (**a**: *n* = 6, **b**: *n* = 7, **c**: *n* = 8), K_2CO_3, DMF, 40–80 °C; (f) Et_3SiOTf, *i*-Pr_2NEt, CH_2Cl_2, 0 °C to rt.

(**1**).[15] The demethylation of **1** with BBr_3 gave 9,10-bis(2,6-dihydroxyphenyl)anthracene (**2**). Finally, the reaction of **2** with 1,*n*-dibromoalkanes (**a**, *n* = 6; **b**, *n* = 7; **c**, *n* = 8) in the presence of K_2CO_3 afforded **3a**, **3b**, and **3c** in 26%, 66%, and 55% yields, respectively. The reaction of **2** with Et_3SiOTf gave quadruple triethylsilyl-protected DPA **4** in 82% yield.[16]

^{1}H NMR Spectra and X-ray Crystal Structures. Figure 1 shows the ^{1}H NMR spectra of **3a–c**, wherein the signals of the

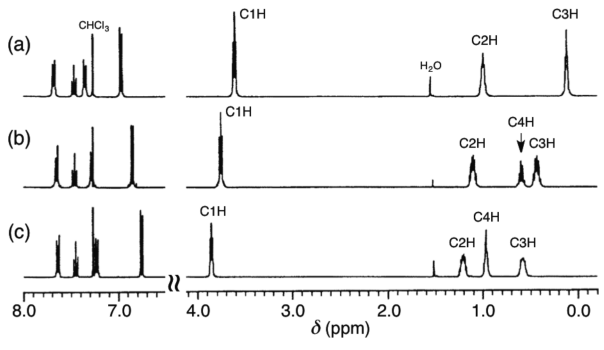

Figure 1. ^{1}H NMR spectra of (a) **3a**, (b) **3b**, and (c) **3c** in $CDCl_3$.

C3H (C4H) of the alkylene strap for **3a**, the C4H for **3b**, and the C4H (C5H) for **3c** are shifted upfield by 1.33, 0.44, and 0.37 ppm, respectively, relative to those of the corresponding 1,*n*-alkanediols, attributable to the ring-current effect of the anthracene ring of **3a–c**. Finally, the molecular structures of **3a–c** and **4** were confirmed by single-crystal X-ray diffraction analyses (Tables S1–S5, Supporting Information).[17] Figure 2 shows that the double alkylene straps in **3a–c** protect the reactive central aromatic ring of the anthracene moiety of DPA, especially the 9,10-positions, and also rigidify the conformation of the diphenyl groups on the DPA. For **4**, quadruple triethylsilyl groups overhang the anthracene moiety. The X-ray packing structures of **3a–c**, **4**, and DPA[18] are shown in Figures S10–S18, Supporting Information.[17] For **3a–c** and **4**,

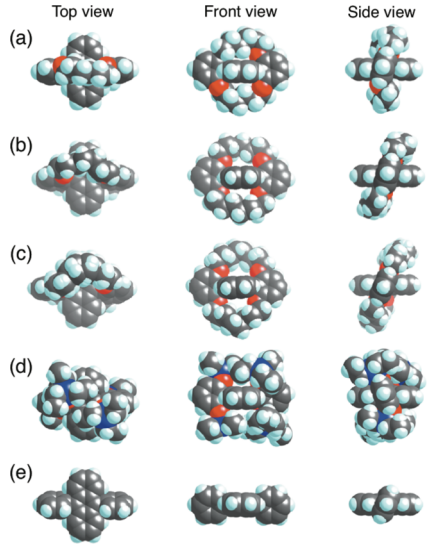

Figure 2. Molecular structures of (a) **3a**, (b) **3b**, (c) **3c**, (d) **4**, and (e) DPA in the X-ray crystal structures. For **3a–c**, two kinds of conformers with different dihedral angles between the anthracene and benzene rings exist in the unit cell,[17] and each one of them is shown here.

neither cofacial π-stacking nor herringbone packing structures were observed, whereas DPA formed a herringbone-like packing structure. The TG–DTA analysis indicated that sublimation begins at around 300 °C for **1**, **3a–c**, and **4** and at around 250 °C for DPA without thermal decomposition (Figure S19, Supporting Information).[17]

UV–vis Absorption Spectra and DFT Calculations. The UV–vis spectra of **1**, **3a–c**, and **4** in THF (or C_6H_{12}) were similar to that of DPA (Figure S20, Supporting Information),[17] wherein the longest wavelength absorption maxima (λ_{max}(abs)) of **1**, **3a–c**, and **4** in THF (or C_6H_{12}) were only slightly red-shifted by 0–4 (0–5) nm relative to the λ_{max}(abs) of DPA (Table S6, Supporting Information).[17] DFT calculations at the B3LYP/6-31G(d) level indicated that the introduction of the double alkylene straps in DPA raises both the HOMO and LUMO energy levels by 0.29 and 0.24 eV for **3a**, 0.36 and 0.33 eV for **3b**, and 0.25 and 0.21 eV for **3c** relative to those of DPA (Figure S21, Supporting Information).[17] However, the HOMO–LUMO gaps of **3a**, **3b**, and **3c** were only slightly reduced by 0.05, 0.03, and 0.04 eV, respectively, relative to that of DPA.

Photostability. The photochemical stability of **1**, **3a–c**, **4**, and DPA was studied under the irradiation of an 18 W fluorescent light (room light) or a 500 W ultrahigh-pressure mercury lamp and air in THF-d_8 or THF, monitored by ^{1}H NMR (2 mM) or UV–vis absorption (0.04 mM) spectroscopies.

Figure 3a shows plots of the ^{1}H NMR signal integration changes of **3b**, **4**, and DPA in THF-d_8 upon exposure to air and an 18 W fluorescent light. Parts Ab,c and Bb,c of Figure 4 also show the ^{1}H NMR spectra for the photochemical changes of **3b** and DPA, respectively, under the same conditions. The double alkylene-strapped DPA **3b** was extremely stable and remained completely intact even after 10 days, and the quadruple triethylsilyl-protected DPA **4** was also fairly stable and remained 79% intact after 10 days. In marked contrast, DPA completely disappeared and changed to the photooxidation product, 9,10-endoperoxide, after 2 days (see also Figure S27B,

dx.doi.org/10.1021/jo302621k | J. Org. Chem. 2013, 78, 2206–2212

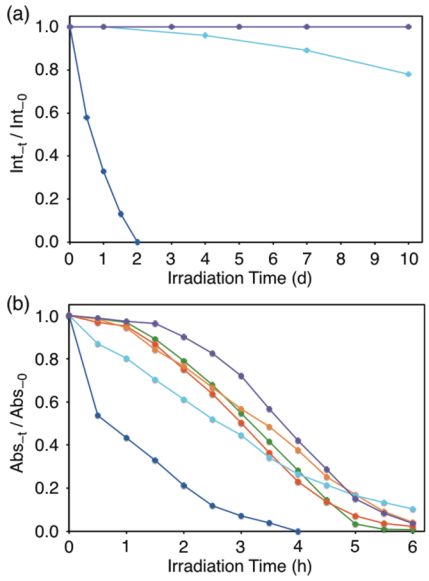

Figure 3. (a) Plots of ^{1}H NMR signal integration changes (Int$_{-t}$/Int$_{-0}$) of **3b** (purple), **4** (light blue), and DPA (blue) (2 mM each) in THF-d_8 as a function of irradiation time (days) upon exposure to air and an 18 W fluorescent light. (b) Plots of the longest wavelength absorption maxima changes (Abs$_{-t}$/Abs$_{-0}$) of **1** (green line), **3a** (red), **3b** (purple), **3c** (orange), **4** (light blue), and DPA (blue) (0.04 mM each) in THF as a function of irradiation time (hours) upon exposure to air and light of a 500 W ultrahigh-pressure mercury lamp.

Supporting Information).[6b,c] Upon exposure to air and the light of a 500 W ultrahigh-pressure mercury lamp, **3b** in THF-d_8 remained almost intact after 1 h (Figure 4Ad) and 56% intact after 6 h irradiation (Figure 4Af). In contrast, DPA almost completely changed to the 9,10-endoperoxide after 1 h (Figure 4Bd), which was completely decomposed to unidentified products after 6 h irradiation (Figure 4Bf). Thus, **3b** was much more resistant to photochemical reactions than DPA, based on the steric protection of the reactive central aromatic ring of the anthracene moiety of **3b** by the double alkylene straps. The detailed ^{1}H NMR spectral changes for the photochemical reactions of **1**, **3a**−**c**, **4**, and DPA (2 mM each) in THF-d_8 are shown in Figures S22−S27 (Supporting Information).[17]

The photochemical stabilities of **1**, **3a**−**c**, **4**, and DPA at high dilution (0.04 mM in THF) upon exposure to air and the light of a 500 W ultrahigh-pressure mercury lamp, monitored by UV−vis absorption spectroscopy (Figure 3b and Figure S28, Supporting Information),[17] were somewhat different from the results under higher concentration conditions (2 mM in THF-d_8) as mentioned above. At high dilution, the photooxidation of DPA was slower because of reduced opportunities for bimolecular reactions. The alkylene straps with ether bonds in **3a**−**c** proved to be not necessarily so robust and **3a**−**c** were completely decomposed to unidentified products after 6 h irradiation. Nevertheless, **3a**−**c** were much more resistant to photochemical reactions than DPA. The photochemical stability in air after 2 h irradiation by the light of a 500 W ultrahigh-pressure mercury lamp was in the order DPA < **4** < **1** ≈ **3a** ≈ **3c** < **3b** (Figure 3b).

Fluorescence Emission Properties. The fluorescence spectra, absolute quantum yields (Φ_F), lifetimes (τ_s), and spectral data of **1**, **3a**−**c**, **4**, and DPA in C_6H_{12}, cast film, powder, and single crystals are shown in Figures 5 and 6a,b and

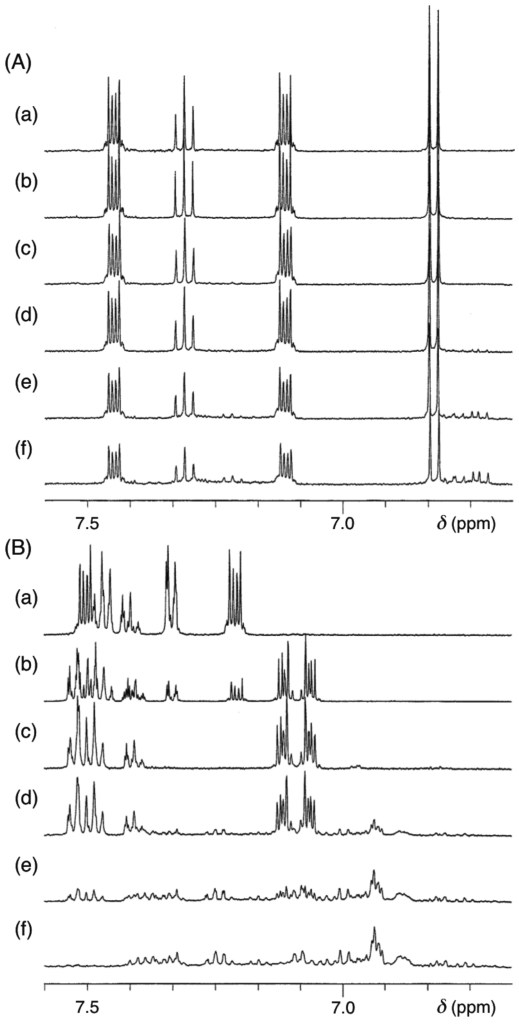

Figure 4. ^{1}H NMR spectra for the photochemical changes of (A) **3b** and (B) DPA (2 mM in THF-d_8) upon exposure to air and light: irradiation of an 18 W fluorescent light for (a) 0 h, (b) 1 d, and (c) 10 d; irradiation of a 500 W ultrahigh-pressure mercury lamp for (d) 1 h, (e) 3 h, and (f) 6 h.

Tables 1 and 2, respectively. The absolute fluorescence quantum yields (Φ_F) were determined by a calibrated integrating sphere system.[19] The fluorescence decays and lifetimes (τ_s) were measured with a time-correlated single photon counting fluorimeter.

In C_6H_{12}, the shortest and the second wavelength fluorescence emission maxima (λ_{max}(em)) of **1** and **3a**−**c** were only slightly blue-shifted relative to that of DPA (Figure 5a and Table 1). The Stokes' shift values of 810, 860, 930, 1050, and 910 cm^{-1} of **1**, **3a**, **3b**, **3c**, and **4**, respectively, were slightly smaller than the 1230 cm^{-1} of DPA (Table S6, Supporting Information),[17] probably reflecting the degree of their conformational rigidity between the anthracene ring and the diphenyl groups at the 9,10-positions. The Φ_F values in C_6H_{12} increased in the order **3a** (Φ_F = 0.93) ≤ **1** (0.94) ≤ **3c** (0.95) ≤ **4** (0.96) ≤ DPA (0.97)[7,19] ≤ **3b** (0.98) (Figure 6a and Table 2).

There are four significant features in the fluorescence properties of **1**, **3a**−**c**, **4**, and DPA *in the solid states (cast film, powder, and single crystals)*.[20,21]

Item 1. In all cases, the λ_{max}(em) values were red-shifted in the order in C_6H_{12} < cast film < powder < single crystals

dx.doi.org/10.1021/jo302621k | J. Org. Chem. 2013, 78, 2206−2212

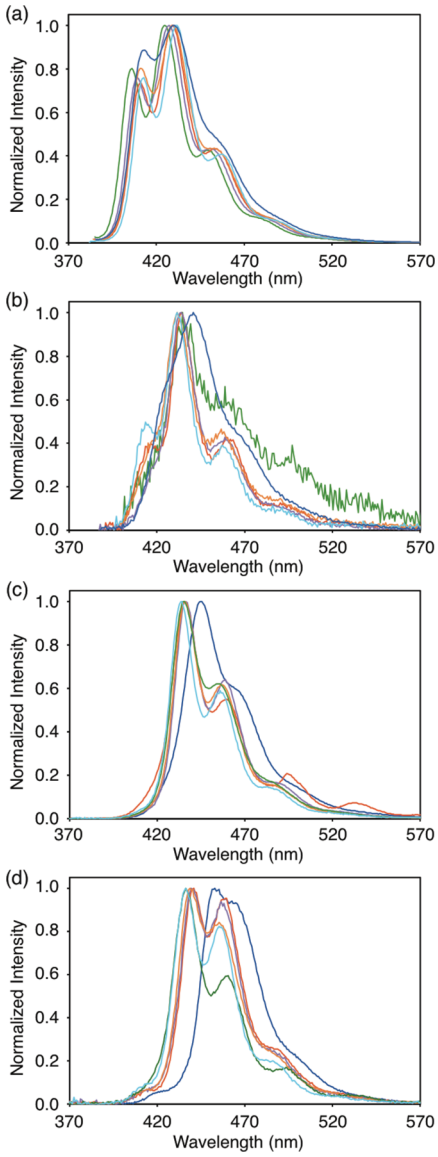

Figure 5. Fluorescence emission spectra of **1** (green line), **3a** (red), **3b** (purple), **3c** (orange), **4** (light blue), and DPA (blue) in (a) C_6H_{12}, (b) cast film, (c) powder, and (d) single crystals.

(Figure 5, Table 1, and Figure S29, Supporting Information),[17] reflecting the exciton coupling in the condensed phase. The difference between the shortest λ_{max}(em) in the single crystals and the second λ_{max}(em) in C_6H_{12} decreased in the order DPA ($\Delta\lambda_{max}$(em) = 23 nm) > **3a** = **3b** (12 nm) ≥ **1** (11 nm) ≥ **3c** (10 nm) > **4** (4 nm).[22] This result reflects the difference in the stacking mode between DPA and other derivatives because of steric hindrance of the substituents at the 2′,6′-positions of the diphenyl groups on DPA.

Item 2. Compounds **1** and **4** in the solid states showed low Φ_F. τ_s of **1** and **4** were shorter than those of **3a**–**c** and DPA in the respective solid state except for **3c** in the powder state. Furthermore, in contrast to **3a**–**c** and DPA, the radiative rate constants (k_f) of **1** and **4** were smaller than their nonradiative rate constants (k_{nr}) (Table 2 and Figure S30, Supporting Information).[17] These results would arise from a thermal vibrational deactivation of the excited states of **1** and **4** with flexible methoxy and triethylsilyloxy groups, respectively.

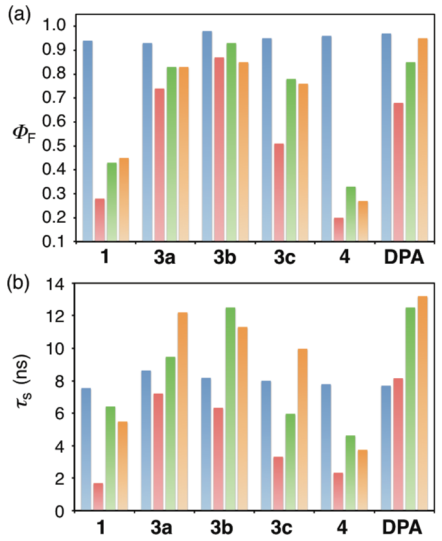

Figure 6. (a) Fluorescence absolute quantum yields (Φ_F) and (b) fluorescence lifetimes (τ_s) of **1**, **3a**–**c**, **4**, and DPA in C_6H_{12} (blue), cast film (red), powder (green), and single crystals (orange).

Table 1. Fluorescence Emission Maxima (λ_{max}(em)) of 1, 3a–c, 4, and DPA in C_6H_{12}, Cast Film, Powder, and the Single Crystals[a]

compd	λ_{max}(em)/nm in C_6H_{12}	λ_{max}(em)/nm in cast film	λ_{max}(em)/nm in powder	λ_{max}(em)/nm in crystals
1	406, 425, (449)	434, 454	436, 455	436, 460
3a	411, 429, 453	(417), 433, 459	436, 460	441, 460
3b	409, 427, 451	(417), 433, 458	436, 459	439, 457
3c	411, 429, 453	(415), 431, 457	436, 457	439, 455
4	413, 432, 457	(414), 431, 457	433, 456	436, 455
DPA	413, 430, (456)	440, (466)	445, 463	453, 466

[a]For sample preparations, see the Experimental Section.

Item 3. For **3a**–**c**, in all solid states of cast film, powder, and single crystals, the Φ_F increased in the order **3c** < **3a** < **3b** (Figure 6a and Table 2). This result would be related to the nature of the double alkylene straps: the C7 strap in **3b** is not tighter than the C6 strap in **3a**, which may strain the excited state of **3a**, and is not looser than the C8 strap in **3c**, which would cause a thermal vibrational deactivation of the excited state of **3c**. *In the cast film and the powder state*, **3b** showed the highest Φ_F of 0.87 and 0.93, respectively, among **1**, **3a**–**c**, **4**, and DPA. Thus, the C7 strap in **3b** effectively blocks fluorescence self-quenching. Surprisingly, *in the single crystals*, DPA exhibited the highest Φ_F among them of 0.95, whereas **3b** showed Φ_F of 0.85. At this stage, it is not easy to elucidate the reason for the paramount Φ_F of DPA in the single crystals, and we must wait for further studies.

Item 4. The τ_s values of **3a** in the single crystals and of both **3b** and DPA in the powder state and the single crystals exceeded 11 ns; these values were greater than those in C_6H_{12} (Table 2). In particular, **3b** in the powder state and DPA in the single crystals showed k_f/k_{nr} = >10, indicating that the radiative process is dominant, similar to that of the emission in C_6H_{12}.

CONCLUSION

We have demonstrated the synthesis and photochemical and photophysical properties of double alkylene-strapped 9,10-

dx.doi.org/10.1021/jo302621k | J. Org. Chem. 2013, 78, 2206–2212

Table 2. Fluorescence Absolute Quantum Yields (Φ_F), Lifetimes (τ_s), Radiative Rate Constants (k_f),[a] and Nonradiative Rate Constants (k_{nr})[a] of 1, 3a−c, 4, and DPA in C_6H_{12}, Cast Film, Powder, and the Single Crystals[b]

compd	Φ_F (τ_s/ns) in C_6H_{12}	k_f/s^{-1}, k_{nr}/s^{-1} in C_6H_{12}	Φ_F (τ_s/ns) in cast film	k_f/s^{-1}, k_{nr}/s^{-1} in cast film	Φ_F (τ_s/ns) in powder	k_f/s^{-1}, k_{nr}/s^{-1} in powder	Φ_F (τ_s/ns) in crystals	k_f/s^{-1}, k_{nr}/s^{-1} in crystals
1	0.94 (7.56)	1.24×10^8, 7.94×10^6	0.28 (1.70)[c]	1.65×10^8, 4.25×10^8	0.43 (6.42)[c]	6.70×10^7, 8.88×10^7	0.45 (5.49)[c]	8.20×10^7, 1.00×10^8
3a	0.93 (8.64)	1.08×10^8, 8.10×10^6	0.74 (7.22)	1.03×10^8, 3.60×10^7	0.83 (9.48)	8.76×10^7, 1.79×10^7	0.83 (12.2)	6.80×10^7, 1.39×10^7
3b	0.98 (8.18)	1.20×10^8, 2.44×10^6	0.87 (6.34)	1.37×10^8, 2.05×10^7	0.93 (12.5)	7.43×10^7, 5.60×10^6	0.85 (11.3)	7.52×10^7, 1.33×10^7
3c	0.95 (8.01)	1.19×10^8, 6.24×10^6	0.51 (3.32)[c]	1.54×10^8, 1.48×10^8	0.78 (5.97)[c]	1.31×10^8, 3.69×10^7	0.76 (9.98)	7.62×10^7, 2.40×10^7
4	0.96 (7.80)	1.23×10^8, 5.13×10^6	0.20 (2.34)	8.57×10^7, 3.43×10^8	0.33 (4.63)[c]	7.13×10^7, 1.45×10^8	0.27 (3.75)[c]	7.20×10^7, 1.95×10^8
DPA	0.97 (7.70)	1.26×10^8, 3.90×10^6	0.68 (8.16)	8.33×10^8, 3.92×10^7	0.85 (12.5)	6.80×10^7, 1.20×10^7	0.95 (13.2)	7.20×10^7, 3.79×10^6

[a] $\Phi_F = k_f/(k_f + k_{nr}) = \tau_s k_f$. [b] For sample preparations, see the Experimental Section. [c] The observed fluorescence decay profiles were analyzed in terms of two exponential decay terms. The intensity-averaged decay time expressed in the Stern−Volmer analyses was used. The detail is shown in ref 19.

diphenylanthracene (DPA) derivatives **3a−c** (**a**: C6 strap, **b**: C7 strap, **c**: C8 strap). In **3a−c**, the reactive central aromatic ring of the anthracene moiety (especially the 9,10-positions of the anthracene ring) is protected by the double alkylene straps. Thus, **3a−c** were much more resistant to photochemical reactions than the parent DPA. The C7 strap in **3b** was not tighter than the C6 strap in **3a** and was not looser than the C8 strap in **3c**. This nature of the C7 strap reflects the chemical yield, photostability, and fluorescence quantum yield (Φ_F) of **3b**. Thus, **3b** exhibited the best performance for photostability in solution and for Φ_F in C_6H_{12}, a cast film, and the powder state among **1**, **3a−c**, **4**, and DPA investigated here, although DPA exhibited the highest Φ_F among them in single crystals. The application of **3b** as a building block for optoelectronics is currently being studied.

EXPERIMENTAL SECTION

General Methods. THF and CH_2Cl_2 were distilled from sodium-benzophenone ketyl and CaH_2, respectively, under an argon atmosphere. The other solvents and all commercially available reagents were used without any purification. ^1H and ^{13}C NMR spectra were recorded at 400 and 100 MHz, respectively. HRMS measurements were performed by EI-TOF-MS. Photoirradiation was conducted with a 500 W ultrahigh-pressure mercury lamp through a heat-absorbing filter.

9,10-Bis(2,6-dimethoxyphenyl)anthracene (1). *Method A.* A solution of 2,6-dimethoxyphenyllithium,[13] which was prepared by the reaction of 1,3-dimethoxybenzene (4.6 mL, 35.1 mmol) in dry THF (80 mL) with a *n*-BuLi hexane solution (1.57 M, 22 mL, 34.5 mmol) at 0 °C for 0.5 h and then at room temperature for 3 h under Ar, was added to a suspension of anthraquinone (2.00 g, 9.61 mmol) in dry THF (40 mL) at −78 °C under Ar. The reaction mixture was allowed to warm to room temperature with stirring overnight and then quenched with H_2O (20 mL) and then 1 M HCl (40 mL) at 0 °C. The precipitate was filtered and washed with H_2O, MeOH, and EtOAc to give 9,10-bis(2,6-dimethoxyphenyl)-9,10-dihydroxyanthracene (pre-**1**) (4.48 g, 96% yield) as a white solid: ^1H NMR ($CDCl_3$, 50 °C) δ 7.35 (dd, J = 3.4 and 5.9 Hz, 4H), 7.21 (s, 2H), 7.20 (t, J = 8.3 Hz, 2H), 7.10 (dd, J = 3.4 and 5.9 Hz, 4H), 6.60 (d, J = 8.3 Hz, 4H), 3.62 (brs, 12H).

To a mixture of pre-**1** (4.45 g, 9.18 mmol), NaI (9.65 g, 64.4 mmol), and $NaH_2PO_2 \cdot H_2O$ (9.73 g, 91.8 mmol) was added AcOH (230 mL).[14] The resulting mixture was stirred at 120 °C for 4 h under Ar and light shielding. After the mixture was cooled to room temperature, the precipitate was filtered and washed with H_2O and MeOH to give **1** (4.01 g, 97% yield) as a white solid: mp 287−288 °C;[15] ^1H NMR ($CDCl_3$) δ 7.62 (dd, J = 3.4 and 6.8 Hz, 4H), 7.51 (t, J = 8.3 Hz, 2H), 7.27 (dd, J = 3.4 and 6.8 Hz, 4H), 6.83 (d, J = 8.3 Hz, 4H), 3.58 (s, 12H); ^{13}C NMR ($CDCl_3$) δ 159.1, 130.4, 129.9, 129.4, 126.7, 124.6, 116.0, 104.3, 56.0; HRMS (EI+) calcd for $C_{30}H_{26}O_4$ 450.1831, found 450.1841.

Method B. To a mixture of 9,10-dibromoanthracene (208 mg, 0.619 mmol), 2,6-dimethoxyphenylboronic acid (450 mg, 2.47 mmol), $Pd(OAc)_2$ (7.0 mg, 0.031 mmol), SPhos (12.8 mg, 0.031 mmol),[13] and K_3PO_4 (527 mg, 2.48 mmol) under Ar were added THF (20 mL) and H_2O (3.2 mL). The resulting mixture was stirred at 60 °C for 69 h under light shielding. After evaporation of solvents, the residue was partitioned between CH_2Cl_2 and H_2O. The organic layer was washed with H_2O and brine and dried over Na_2SO_4. After evaporation of solvent, the residue was purified by column chromatography on silica gel eluted with CH_2Cl_2−hexane (1:3) followed by reprecipitation with CH_2Cl_2−hexane to give **1** (180 mg, 65% yield) as a white solid.

9,10-Bis(2,6-dihydroxyphenyl)anthracene (2). To a solution of **1** (2.59 g, 5.75 mmol) in dry CH_2Cl_2 (280 mL) at −78 °C under N_2 and light shielding was added dropwise a solution of BBr_3 (2.3 mL, 23.9 mmol) in dry CH_2Cl_2 (20 mL) over a period of 5 min. The reaction mixture was allowed to warm to room temperature with stirring overnight. After additional stirring at room temperature for 24

dx.doi.org/10.1021/jo302621k | J. Org. Chem. 2013, 78, 2206−2212

h, the reaction mixture was poured into ice-cold water and neutralized with $NaHCO_3$. After evaporation of most of the CH_2Cl_2, the mixture was extracted with EtOAc. The organic layer was washed with H_2O and brine and dried over Na_2SO_4. After evaporation of solvents, the residue was purified by reprecipitation with THF−hexane to give **2** (2.00 g, 88% yield) as a pale yellow solid: mp 322 °C dec; ^{1}H NMR (DMSO-d_6, 80 °C) δ 8.98 (s, 4H), 7.58 (dd, J = 3.4 and 6.8 Hz, 4H), 7.29 (dd, J = 3.4 and 6.8 Hz, 4H), 7.15 (t, J = 8.3 Hz, 2H), 6.57 (d, J = 8.3 Hz, 4H); ^{13}C NMR (DMSO-d_6, 80 °C) δ 156.9, 130.6, 130.1, 128.9, 126.8, 124.3, 111.9, 106.4; HRMS (EI+) calcd for $C_{26}H_{18}O_4$ 394.1205, found 394.1239.

Typical Procedure for the Synthesis of Double Alkylene-Strapped Diphenylanthracenes (3): C7 Strap DPA (3b). To a mixture of **2** (240 mg, 0.608 mmol) and K_2CO_3 (420 mg, 3.04 mmol) were added DMF (120 mL) and 1,7-dibromoheptane (220 μL, 1.29 mmol). The reaction mixture was stirred at 40 °C for 24 h and then at 80 °C for 48 h under Ar and light shielding. After evaporation of solvent, the residue was partitioned between CH_2Cl_2 and H_2O. The organic layer was washed with H_2O and brine and dried over Na_2SO_4. After evaporation of solvent, the residue was purified by column chromatography on silica gel eluted with CH_2Cl_2−hexane (1:3) followed by reprecipitation with CH_2Cl_2−hexane to give **3b** (235 mg, 66% yield) as a white solid: mp 279−281 °C; ^{1}H NMR ($CDCl_3$) δ 7.65 (dd, J = 3.4 and 6.8 Hz, 4H), 7.46 (t, J = 8.3 Hz, 2H), 7.28 (dd, J = 3.4 and 6.8 Hz, 4H), 6.86 (d, J = 8.3 Hz, 4H), 3.76 (t, J = 5.4 Hz, 8H), 1.10 (quint, J = 5.4 Hz, 8H), 0.60 (br quint, J = 6.8 Hz, 4H), 0.43 (quint, J = 7.3 Hz, 8H); ^{13}C NMR ($CDCl_3$) δ 159.0, 130.4, 130.1, 129.3, 126.8, 124.2, 119.5, 108.1, 69.9, 29.0, 27.8, 24.8; HRMS (EI+) calcd for $C_{40}H_{42}O_4$ 586.3083, found 586.3056.

C6 Strap DPA (3a): white solid; 26% yield; mp 286−288 °C; ^{1}H NMR ($CDCl_3$) δ 7.68 (dd, J = 3.4 and 6.8 Hz, 4H), 7.47 (t, J = 8.3 Hz, 2H), 7.35 (dd, J = 3.4 and 6.8 Hz, 4H), 6.97 (d, J = 8.3 Hz, 4H), 3.61 (t, J = 5.4 Hz, 8H), 1.00 (quint, J = 5.4 Hz, 8H), 0.11 (br quint, J = 2.9 Hz, 8H); ^{13}C NMR ($CDCl_3$) δ 159.2, 130.3, 130.2, 129.7, 126.8, 125.0, 123.0, 113.2, 72.3, 30.1, 25.6; HRMS (EI+) calcd for $C_{38}H_{38}O_4$ 558.2770, found 558.2747.

C8 Strap DPA (3c): white solid; 55% yield; mp 277−279 °C; ^{1}H NMR ($CDCl_3$) δ 7.64 (dd, J = 3.4 and 6.8 Hz, 4H), 7.45 (t, J = 8.3 Hz, 2H), 7.23 (dd, J = 3.4 and 6.8 Hz, 4H), 6.76 (d, J = 8.3 Hz, 4H), 3.85 (t, J = 5.4 Hz, 8H), 1.21 (m, 8H), 0.96 (m, 8H), 0.58 (m, 8H); ^{13}C NMR ($CDCl_3$) δ 158.7, 130.3, 129.8, 129.1, 127.2, 123.9, 115.5, 104.0, 68.5, 28.8, 26.9, 23.4; HRMS (EI+) calcd for $C_{42}H_{46}O_4$ 614.3396, found 614.3375.

9,10-Bis[2,6-bis(triethylsilyloxy)phenyl]anthracene (4). To a suspension of **2** (180 mg, 0.456 mmol) in dry CH_2Cl_2 (12 mL) at 0 °C under Ar and light shielding were added i-Pr_2NEt (700 μL, 4.02 mmol) and Et_3SiOTf (620 μL, 2.74 mmol). The reaction mixture was stirred at 0 °C for 2 h and then at room temperature for 48 h. The resulting mixture was quenched with H_2O at 0 °C and extracted with CH_2Cl_2. The organic layer was washed with H_2O and brine and dried over Na_2SO_4. After evaporation of solvent, the residue was purified by column chromatography on silica gel eluted with CH_2Cl_2−hexane (1:10) to give **4** (318 mg, 82% yield) as a white solid: mp 130−131 °C; ^{1}H NMR ($CDCl_3$) δ 7.67 (dd, J = 3.4 and 6.8 Hz, 4H), 7.28−7.20 (m, 6H), 6.68 (d, J = 8.3 Hz, 4H), 0.55 (t, J = 7.8 Hz, 36H), 0.35 (q, J = 7.8 Hz, 24H); ^{13}C NMR ($CDCl_3$) δ 155.7, 130.2 (two coincident resonances), 128.3, 127.5, 123.8, 121.2, 111.1, 6.3, 4.9; HRMS (EI+) calcd for $C_{50}H_{74}O_4Si_4$ 850.4664, found 850.4660.

Fluorescence Studies. The absolute fluorescence quantum yields (Φ_F) were determined by a calibrated integrating sphere system.[19] The fluorescence decays and lifetimes (τ_s) were measured with a time-correlated single photon counting fluorimeter.

Before measurements, **1**, **3a−c**, **4**, and DPA were purified by column chromatography on silica gel, then by recycle preparative HPLC using a polystyrene gel column, and finally by reprecipitation. The sample preparation methods were as follows.[21] In a N_2-saturated C_6H_{12}, the concentration was 1.0×10^{-5} M for **1** and 2.4×10^{-5} M for **3a−c**, **4**, and DPA. Drop cast films were prepared from one drop of a 100 μL microsyringe of a 1 mM CH_2Cl_2 solution of sample. Powders were prepared by reprecipitation from CH_2Cl_2−hexane for **1**, **3a−c**, and DPA and from hexane−EtOH for **4**. Single crystals were prepared by recrystallization from a hot benzene−hexane solution for **1**, **3a−c**, and DPA and recrystallization by slow diffusion of EtOH into a hexane solution of **4**. These manipulations were carried out under the extinction of room light.

X-ray Data Collection and Crystal Structure Determination of 3a−c, 4, and DPA. The data were measured by using a CCD area detector, using Mo−Kα graphite monochromated radiation (λ = 0.71073 Å). The structures were solved by direct methods using the program SHELXS-97.[23] The refinements and all further calculations were carried out by using SHELXL-97.[23] The H-atoms were included in calculated positions and treated as riding atoms by using the SHELXL default parameters. The non-H atoms were refined anisotropically, using weighted full-matrix least-squares on F^2. Crystal data and structure refinements are listed in Tables S1−S5 (Supporting Information), and ORTEP views are shown in Figure S9 in the Supporting Information. Crystallographic data (excluding structure factors) for the structure in this paper have been deposited with the Cambridge Crystallographic Data Centre as supplementary publication nos. CCDC 911869 for **3a**, CCDC 911870 for **3b**, CCDC 911871 for **3c**, CCDC 911872 for **4**, and CCDC 911873 for DPA.

■ ASSOCIATED CONTENT

Ⓢ Supporting Information

Additional spectral data of **1**, **3a−c**, **4**, and DPA and ORTEP views, crystal packing structures, and X-ray crystallographic data (CIF) of **3a−c**, **4**, and DPA. This material is available free of charge via the Internet at http://pubs.acs.org.

■ AUTHOR INFORMATION

Corresponding Author

*E-mail: skkobay@ipc.shizuoka.ac.jp.

Notes

The authors declare no competing financial interest.

■ ACKNOWLEDGMENTS

This work was supported in part by a Grant-in-Aid from JSPS (No. 22350060).

■ REFERENCES

(1) (a) Kim, Y.-H.; Shin, D.-C.; Kim, S.-H.; Ko, C.-H.; Yu, H.-S.; Chae, Y.-S.; Kwon, S.-K. *Adv. Mater.* **2001**, *13*, 1690−1693. (b) Hung, L. S.; Chen, C. H. *Mater. Sci. Eng., R* **2002**, *39*, 143−222. (c) Kim, Y.-H.; Jeong, H.-C.; Kim, S.-H.; Yang, K.; Kwon, S.-K. *Adv. Funct. Mater.* **2005**, *15*, 1799−1805. (d) Lyu, Y.-Y.; Kwak, J.; Kwon, O.; Lee, S.-H.; Kim, D.; Lee, C.; Char, K. *Adv. Mater.* **2008**, *20*, 2720−2729. (e) Vinyard, D. J.; Su, S.; Richter, M. M. *J. Phys. Chem. A* **2008**, *112*, 8529−8533. (f) Moorthy, J. N.; Venkatakrishnan, P.; Natarajan, P.; Huang, D.-F.; Chow, T. J. *J. Am. Chem. Soc.* **2008**, *130*, 17320−17333. (g) Nakanishi, W.; Hitosugi, S.; Piskareva, A.; Shimada, Y.; Taka, H.; Kita, H.; Isobe, H. *Angew. Chem., Int. Ed.* **2010**, *49*, 7239−7242.

(2) (a) Yang, W. J.; Kim, C. H.; Jeong, M.-Y.; Lee, S. K.; Piao, M. J.; Jeon, S.-J.; Cho, B. R. *Chem. Mater.* **2004**, *16*, 2783−2789. (b) Yang, W. J.; Seo, M. S.; Wang, X. Q.; Jeon, S.-J.; Cho, B. R. *J. Fluoresc.* **2008**, *18*, 403−411. (c) Ji, S.; Wu, W.; Wu, W.; Guo, H.; Zhao, J. *Angew. Chem., Int. Ed.* **2011**, *50*, 1626−1629.

(3) (a) Ito, K.; Suzuki, T.; Sakamoto, Y.; Kubota, D.; Inoue, Y.; Sato, F.; Tokito, S. *Angew. Chem., Int. Ed.* **2003**, *42*, 1159−1162. (b) Meng, H.; Sun, F.; Goldfinger, M. B.; Gao, F.; Londono, D. J.; Marshall, W. J.; Blackman, G. S.; Dobbs, K. D.; Keys, D. E. *J. Am. Chem. Soc.* **2006**, *128*, 9304−9305. (c) Zhao, Q.; Kim, T. H.; Park, J. W.; Kim, S. O.; Jung, S. O.; Kim, J. W.; Ahn, T.; Kim, Y.-H.; Yi, M. H.; Kwon, S.-K. *Adv. Mater.* **2008**, *20*, 4868−4872.

(4) For FET property of DPA, see: (a) Tripathi, A. K.; Heinrich, M.; Siegrist, T.; Pflaum, J. *Adv. Mater.* **2007**, *19*, 2097−2101. (b) Zhang, X.; Yuan, G.; Li, Q.; Wang, B.; Zhang, X.; Zhang, R.; Chang, J. C.; Lee, C.-S.; Lee, S.-T. *Chem. Mater.* **2008**, *20*, 6945−6950.

(5) Marrocchi, A.; Silvestri, F.; Seri, M.; Facchetti, A.; Taticchia, A.; Marks, T. J. *Chem. Commun.* **2009**, 1380−1382.
(6) (a) Bouas-Laurent, H.; Castellan, A.; Desvergne, J.-P.; Lapouyade, R. *Chem. Soc. Rev.* **2001**, *30*, 248−263. (b) Aubry, J.-M.; Pierlot, C.; Rigaudy, J.; Schmidt, R. *Acc. Chem. Res.* **2003**, *36*, 668−675. (c) Zehm, D.; Fudickar, W.; Linker, T. *Angew. Chem., Int. Ed.* **2007**, *46*, 7689−7692.
(7) Iida, A.; Yamaguchi, S. *Chem. Commun.* **2009**, 3002−3004 and references cited therein.
(8) For protection of photoreactive organic dyes and an anthracene derivative by rotaxane encapsulations, see: (a) Frampton, M. J.; Anderson, H. L. *Angew. Chem., Int. Ed.* **2007**, *46*, 1028−1064. (b) Stone, M. T.; Anderson, H. L. *Chem. Commun.* **2007**, 2387−2389.
(9) For protection of anthracene derivatives by the encapsulation in self-assembled capsules, see: (a) Kaanumalle, L. S.; Gibb, C. L. D.; Gibb, B. C.; Ramamurthy, V. *J. Am. Chem. Soc.* **2005**, *127*, 3674−3675. (b) Nishimura, N.; Kobayashi, K. *J. Org. Chem.* **2010**, *75*, 6079−6085.
(10) For alkylene-strapped porphyrins, see: (a) Konishi, K.; Yahara, K.; Toshishige, H.; Aida, T.; Inoue, S. *J. Am. Chem. Soc.* **1994**, *116*, 1337−1344. (b) Sugiyasu, K.; Takeuchi, M. *Chem.—Eur. J.* **2009**, *15*, 6350−6362. (c) Lee, C.-H.; Galoppini, E. *J. Org. Chem.* **2010**, *75*, 3692−3704.
(11) For alkylene-strapped π-conjugated ladder polymers, see: (a) Schlüter, A.-D.; Löffler, M.; Enkelmann, V. *Nature* **1994**, *368*, 831−834. (b) Fiesel, R.; Huber, J.; Scherf, U. *Angew. Chem., Int. Ed. Engl.* **1996**, *35*, 2111−2113.
(12) For double alkylene-strapped bithiophene and its polymer, see: (a) Sugiyasu, K.; Honsho, Y.; Harrison, R. M.; Sato, A.; Yasuda, T.; Seki, S.; Takeuchi, M. *J. Am. Chem. Soc.* **2010**, *132*, 14754−14756. (b) Ouchi, Y.; Sugiyasu, K.; Ogi, S.; Sato, A.; Takeuchi, M. *Chem.-Asian J.* **2012**, *7*, 75−84.
(13) Barder, T. E.; Walker, S. D.; Martinelli, J. R.; Buchwald, S. L. *J. Am. Chem. Soc.* **2005**, *127*, 4685−4696.
(14) Kaur, I.; Miller, G. P. *New J. Chem.* **2008**, *32*, 459−463.
(15) Zweig, A.; Maurer, A. H.; Roberts, B. G. *J. Org. Chem.* **1967**, *32*, 1322−1329.
(16) The reaction of **2** with *t*-BuMe_2SiOTf and *i*-Pr_3SiOTf did not produce quadruple trialkylsilyl-protected DPAs.
(17) See the Supporting Information.
(18) For the X-ray crystallographic analysis of DPA, see also: (a) Langer, V.; Becker, H.-D. *Z. Kristallogr.* **1992**, *199*, 313−315. (b) Reference 4.
(19) Suzuki, K.; Kobayashi, A.; Kaneko, S.; Takehira, K.; Yoshihara, T.; Ishida, H.; Shiina, Y.; Oishi, S.; Tobita, S. *Phys. Chem. Chem. Phys.* **2009**, *11*, 9850−9860.
(20) For size dependence of fluorescence quantum yield in the crystalline state, see: (a) Reference 7. (b) Katoh, R.; Suzuki, K.; Furube, A.; Kotani, M.; Tokumaru, K. *J. Phys. Chem. C* **2009**, *113*, 2961−2965.
(21) The polarizing microscope observations suggested that the cast film and powdery samples are amorphous or polycrystal. The quantum yields in the cast film, powder state, and single crystals were reproduced within ± 0.02 under the sample preparation conditions mentioned in the Experimental Section.
(22) In all cases, the shortest λ_{max}(em) in C_6H_{12} were almost absent in the solid states, as shown in Figure 5. A similar phenomenon is known for DPA in C_6H_{12}, wherein the intensity of the shortest λ_{max}(em) of DPA in C_6H_{12} decreases with increasing the concentration.[19]
(23) Sheldrick, G. M. *SHELXS-97* and *SHELXL-97*, University of Göttingen, Göttingen, Germany, 1997.